Neurosci. Bull. July, 2023, 39(7):1131–1145
https://doi.org/10.1007/s12264-022-01004-7

www.neurosci.cn
www.springer.com/12264

ORIGINAL ARTICLE

Inhibition of *Foxp4* Disrupts Cadherin-based Adhesion of Radial Glial Cells, Leading to Abnormal Differentiation and Migration of Cortical Neurons in Mice

Xue Li[1,2] · Shimin Zou[1,2] · Xiaomeng Tu[1,2] · Shishuai Hao[1,2] · Tian Jiang[3] · Jie-Guang Chen[1,2]

Received: 9 June 2022 / Accepted: 4 September 2022 / Published online: 16 January 2023

Abstract Heterozygous loss-of-function variants of *FOXP4* are associated with neurodevelopmental disorders (NDDs) that exhibit delayed speech development, intellectual disability, and congenital abnormalities. The etiology of NDDs is unclear. Here we found that FOXP4 and N-cadherin are expressed in the nuclei and apical end-feet of radial glial cells (RGCs), respectively, in the mouse neocortex during early gestation. Knockdown or dominant-negative inhibition of *Foxp4* abolishes the apical condensation of N-cadherin in RGCs and the integrity of neuroepithelium in the ventricular zone (VZ). Inhibition of *Foxp4* leads to impeded radial migration of cortical neurons and ectopic neurogenesis from the proliferating VZ. The ectopic differentiation and deficient migration disappear when *N-cadherin* is over-expressed in RGCs. The data indicate that *Foxp4* is essential for N-cadherin-based adherens junctions, the loss of which leads to periventricular heterotopias. We hypothesize that *FOXP4* variant-associated NDDs may be caused by disruption of the adherens junctions and malformation of the cerebral cortex.

Keywords Neurogenesis · Radial migration · Radial glial cell · Ventricular zone · N-cadherin

Introduction

The forkhead box P (FOXP) transcription factors are a group of evolutionarily ancient proteins. In mammals, the FOXP subfamily consists of four members: FOXP1–4. They share a conserved zinc finger domain, a leucine zipper motif, and a forkhead DNA-binding module. FOXP1, FOXP2, and FOXP4 form homodimers or heterodimers for transcriptional regulation and exhibit overlapping, but distinct, expression patterns within the vertebrate brain [1, 2]. Loss-of-function *FOXP* variants have been found in patients with neurodevelopmental disorders (NDDs). For example, *FOXP2* was the first gene discovered to underlie a rare inherited speech and language disorder [3, 4]. *De novo* mutations of *FOXP1* have been linked to a wide spectrum of cognitive disorders, including intellectual disability, speech impairments, and autism [5–7]. In animal studies, ablation of cortical *Foxp2* alters social behavior [8], while conditional knockout of *Foxp1* in the brain results in autistic-like behaviors in mice [9], supporting the hypothesis that the loss of *Foxp1* or *Foxp2* contributes to NDDs. More recently, heterozygous loss-of-function variants in *FOXP4* have been found in children with autosomal dominant NDDs who exhibit speech/language delays and variable congenital abnormalities. The missense mutations of *FOXP4* occur in the forkhead DNA binding domain, resulting in loss of the transcription repression capability but not the interaction with wild-type (WT) FOXP4 protein [10]. However, the neural mechanism by which the loss-of-function mutants of *FOXP4* result in NDDs remains to be determined.

Xue Li, Shimin Zou, and Xiaomeng Tu contributed equally to this work.

✉ Jie-Guang Chen
jiesbooks@gmail.com; jgchen@mail.eye.ac.cn

[1] School of Ophthalmology and Optometry and Eye Hospital, Wenzhou Medical University, Wenzhou 325027, China

[2] State Key Laboratory of Optometry, Ophthalmology and Vision Science, and Zhejiang Provincial Key Laboratory of Optometry and Ophthalmology, Wenzhou 325027, China

[3] Research Center for Translational Medicine, the Affiliated Wenling Hospital of Wenzhou Medical University, Wenling 317500, China

The neocortex, responsible for higher-order brain functions, is the primary site of the pathological changes causing NDDs. The development of the mammalian cerebral cortex starts with the apical neural progenitors that comprise pseudostratified neuroepithelium, a cellular layer residing in the luminal side of the ventricular zone (VZ) in the dorsal telencephalon. In early gestation, the neural progenitors of the neocortex divide symmetrically to expand the progenitor pool. As neurogenesis progresses, the apical neural progenitors begin to give rise to either an excitatory neuron or a basal progenitor cell (BPC). The BPC moves to the subventricular zone (SVZ) and gives rise to pairs of differentiated neurons. After birth, the post-mitotic neurons migrate radially toward the meninges [11]. The early-generated neurons occupy the deepest layer, whereas the late-born neurons migrate to the superficial layers, forming a complex six-layered ''inside-out'' architecture [12]. Neurons in the different laminae have distinct molecular characteristics, reflecting their time of generation. The migration and final laminar positioning of cortical neurons are regulated by cell type- and layer-specific transcription factors [13]. Both *Foxp1* and *Foxp2* are essential for the neurogenesis and radial migration of cortical neurons [14–17]. Disruption of the laminar structure due to defective migration leads to severe neurological disorders, such as lissencephaly and periventricular heterotopias [18].

The apical neural progenitors are also called radial glial cells (RGCs) because of their highly polarized morphology, extending a short apical process and a longer basal (radial) process spanning the neocortex. The migration of cortical neurons requires RGCs; the radial process of RGCs provides an instructive scaffold for migrating neurons to move toward the cortical plate (CP) [19]. Homophilic interactions between N-cadherin proteins located in the plasma membrane of the RGC and the neuron support the neuronal adhesion to the radial glial fiber is essential for radial migration [20]. On the other hand, the apical processes of RGCs form end-feet that connect the neighboring RGCs *via* N-cadherin-mediated adherens junctions (AJs) on the luminal surface of the VZ [21]. Cadherin-based AJs play an obligate role in maintaining neuroepithelial cohesion and confine polarity proteins to appropriate membrane compartments for the polarized RGCs, thereby governing the integrity of the ventricular wall and neuronal migration [22, 23]. Furthermore, the N-cadherin-based AJs provide a self-supportive niche and control the self-renewal of the neural progenitors. Blocking the functioning or knockdown of N-cadherin induces premature neuronal differentiation and inhibits β-catenin signaling in the VZ [24]. β-catenin is an intracellular binding partner for N-cadherin in the AJs and, at the same time, plays a critical role in the proliferative activity of the Wnt signaling pathway [24, 25]. The precise molecular and cellular mechanisms responsible for maintaining N-cadherin-based AJs in the radial glial structures are not fully understood. The expression of N-cadherin in the neuroepithelium of the developing spinal cord is subject to the regulation of forkhead transcription factors. Elevated expression of either *Foxp2* or *Foxp4* represses the *N-cadherin* and disrupts the AJs of the neuroepithelium, leading to premature neurogenesis in the VZ and luminal surface [26]. Mutations in genes known to control AJ formation cause a group of inherited cortical malformations characterized as neuronal heterotopias [27–29].

In this study, we investigated the neural mechanisms responsible for the NDD associated with loss-of-function *FOXP4* mutants in mice. We found that knockdown or dominant-negative inhibition of *Foxp4* disrupted N-cadherin-dependent adhesion between the RGCs, and led to ectopic neurogenesis and defective radial migration in the developing cerebral cortex. We hypothesize that the NDDs associated with *FOXP4* variants may be caused by the disruption of N-cadherin-based adhesion and the resulting malformation of the cerebral cortex.

Materials and Methods

Animals

CD1 mice were purchased from Shanghai Jisijie Laboratory Animal Co., Ltd. The mice were housed under a standard 12 h light-dark cycle and given *ad libitum* access to water and chow. The morning on which a vaginal plug was observed in female mice was counted as embryonic day 0.5 (E0.5) for the fetuses, and the day of birth was considered postnatal day 0 (P0). All experiment procedures and husbandry were performed strictly in compliance with the animal handling guidelines and protocol approved by the Animal Care Committee of Wenzhou Medical University.

Plasmids

Foxp4 shRNAs were constructed and inserted into pSUPER using BglII and HindIII sites. The interfering short-hairpin RNA-expressing constructs shFoxp4-1 and shFoxp4-2 targeted the mouse *Foxp4* coding regions: 5′-GCTGACGCT AAATGAGATTTA-3′ and 5′-CAGAGCTGGAAACGA TGAGAT-3′, respectively. Control scrambled shRNA (shFoxp4-sc) targeting GGAAACCTATTGTCGGATAAT, which has no mouse target genes by blast search, was cloned into pSUPER as a negative control. The full-length *Foxp4* and *N-cadherin* were PCR amplified from a mouse brain complementary DNA library. Mouse Foxp4-H522N carrying a point mutation of *Foxp4* was generated from wild-type

(WT) *Foxp4* using the Fast Site-Directed Mutagenesis Kit (Tiangen Biotech, KM101). WT *Foxp4* and Foxp4-H522N were cloned into the pCAGEN vector (Addgene) using EcoRV and NotI restriction sites. All plasmids used in this study were verified by sequencing and extracted using the EndoFree Plasmid kit (Qiagen).

In utero Electroporation (IUE)

E14.5 ICR female mice were used for IUE [30]. Timed-pregnant mice were anesthetized by intraperitoneal injection of pentobarbital sodium (50 mg/kg body weight, Miaodi, Shanghai, China) diluted in saline. A midline abdominal incision of ~1.5 cm was made, and the uterine horns were carefully exposed. Plasmid DNA solutions containing 0.01% fast green were injected into the lateral ventricles of embryos with a glass micropipette. Electrical pulses (40 V for 50 ms, five times, 950 ms intervals) were applied to the head of embryos in the uterus through forceps-type electrodes connected to an electroporator (BTX, ECM830). Subsequently, the uterus was placed back, and the abdomen was sutured. The mice were sacrificed at indicated times following IUE to collect the electroporated brains for experiments.

Immunofluorescence of Brain Slices

The brains were dissected and fixed in 4% paraformaldehyde in phosphate buffer (PBS, 0.1 M) at 4°C for 4–6 h. Samples were cryoprotected in 30% sucrose and frozen in OCT compound (Thermo, 6502). Cryosections at 14 μm were cut in the coronal plane on a cryostat (HM505E, Microm, Germany). Heat-mediated antigen retrieval was conducted by incubating the slides in citrate buffer (10 mM citrate, pH 6, 0.05% Tween-20) for 5 min at 100°C. Sections were blocked with PBS containing 0.3 % Triton X-100, 1% BSA, and 5% donkey normal serum. After overnight incubation at 4°C with the primary antibody, the sections were rinsed in PBS and incubated with the appropriate secondary antibodies. The following primary antibodies and dilutions were used: goat anti-GFP (1:500, Novus NB100-1770); rabbit anti-FOXP4 (1:150, Abcam, ab242127); mouse anti-FOXP1 (1:250, Santa Cruz, sc-398811); rabbit anti-nestin (1:600, Abcam, ab221660); mouse anti-N-cadherin (1:100, Santa Cruz, sc-59987); rabbit anti-β-catenin (1:200, Abcam, ab32572); rabbit anti-SATB2 (1:500, Abcam, ab92446); mouse anti-FOXP4 (1:100, Santa Cruz, sc-390892); mouse anti-SOX2 (1:100, Santa Cruz, sc-365823); rabbit anti-TBR1 (1:400, Abcam, ab31940); rabbit anti-TBR2 (1:400, Abcam, ab23345); and mouse anti-phospho Histone H3 (pH3) (1:300, Abcam, ab14955). The species-specific secondary antibodies applied in this study were from Jackson ImmunoResearch Laboratories. They were: Alexa Fluor™488-conjugated anti-goat, anti-mouse, and anti-rabbit IgGs (1:500); Cy3-conjugated anti-rabbit (1:500); Alexa Fluor™594-conjugated anti-mouse and anti-rabbit IgG (1:500); and Alexa Fluor™647-conjugated anti-rabbit and anti-mouse IgGs (1:500). The sections were mounted with an anti-fade mounting medium (Invitrogen, S36938) that contained DAPI for nuclear staining.

Image Acquisition and Statistical Analysis

Images were acquired using a Zeiss LSM 880 confocal microscope. The fluorescence intensity of N-cadherin along the ventricular surface in the transfected cortical region was calculated by ImageJ and expressed as a percentage of the scrambled control, assuming the control to be 100%. Data from at least three independent experiments were used for analysis. Results are reported as the mean ± SEM. A paired or unpaired Student's *t*-test was applied to compare the difference between the control and experimental groups using Graphpad Prism 8. Multiple comparisons were analyzed by one-way ANOVA, followed by Tukey's *post hoc* multiple comparisons test. $P < 0.05$ was defined as statistically significant. Asterisks indicate *p* values with $*P < 0.05$, $**P < 0.01$, and $***P < 0.001$.

Results

Foxp4 is Expressed in the Developing Cerebral Cortex

During the embryonic development of the rat cerebral cortex, the *Foxp4* mRNA signal is detected in the VZ/SVZ and CP by E14 and later in all cortical layers. The expression of *Foxp4* declines gradually in the early postnatal cortex [31]. In this study, we examined *Foxp4* expression in developing mouse brains by immunofluorescence. At E12.5, the *Foxp4* was broadly expressed in the VZ, SVZ, and pre-plate. At E14.5, FOXP4 staining was found across all layers of the developing cortex, from the VZ/SVZ to the CP. Peak expression of *Foxp4* occurred in the intermediate zone (IZ), where early-born neurons were migrating toward the pial surface. *Foxp4* expression in the IZ was largely reduced at E16.5. At P0, *Foxp4* was found in the CP and SVZ but not in the VZ. Thus, *Foxp4* exhibited diminished expression in the germinal zone as cortical neurogenesis was completed (Fig. 1A). We also determined the identities of $FOXP4^+$ cells by double labeling of FOXP4 with various cell-type-specific markers in the E14.5 mouse cortex. As a transcription factor, FOXP4 protein was found in the cell nuclei, where it co-localized with $SOX2^+$ (a marker of RGCs) in the VZ, and $TBR2^+$ (a marker of basal progenitors) in the SVZ/IZ. In the CP, FOXP4 was enriched in the $TBR1^+$ cells that were immature post-mitotic neurons (Fig. 1B). The expression profile indicated that *Foxp4* may play multiple roles during cortical development.

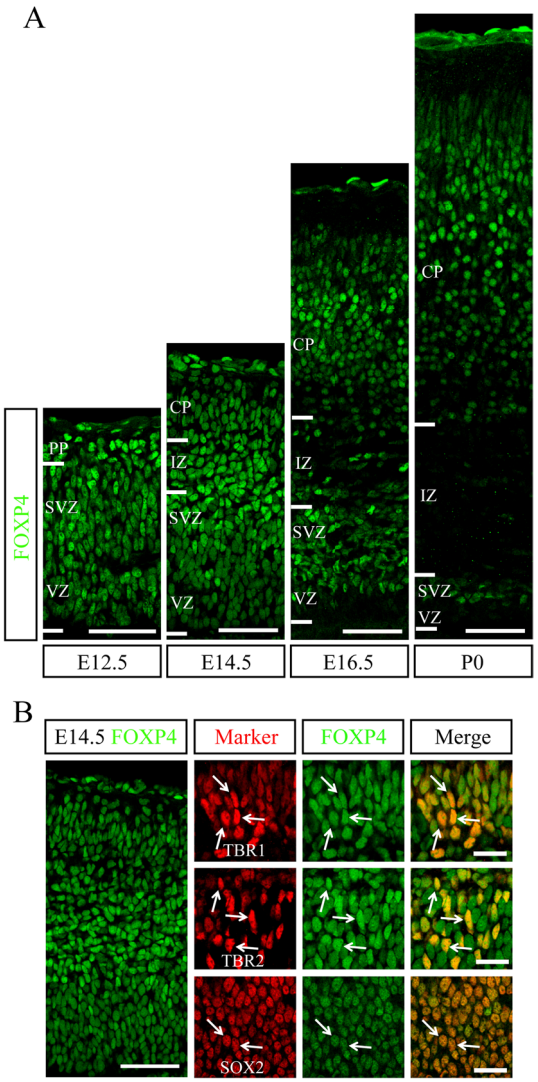

Fig. 1 Expression of *Foxp4* in mouse neocortex during development. **A** Immunostaining for FOXP4 (green) and DAPI on coronal sections at E12.5, E14.5, E16.5, and P0. PP, pre-plate; CP, cortical plate; SVZ, subventricular zone; VZ, ventricular zone; IZ, intermediate zone. DAPI staining of nuclei is omitted from the figures for clarity. Scale bars, 50 μm. **B** Representative images of E14.5 neocortical sections double immunostained for FOXP4 (green) and the indicated cell-type markers (red). FOXP4 is co-localized with SOX2, TBR2, and TBR1 (arrows). Scale bars, 50 μm in the left and 20 μm in the magnified images.

Knockdown of *Foxp4* Results in Abnormal Positioning of Cortical Cells

To gain insight into the possible role of *Foxp4*, we set out to investigate its functional importance in neuronal development by knocking down *Foxp4* expression. We designed two short hairpin RNA (shRNA) constructs targeting distinct regions of the *Foxp4* coding sequence (hereafter designated as shFoxp4-1 and shFoxp4-2) and a scrambled vector (shFoxp4-sc) as the control. To test the knockdown (KD) efficiency of the shRNA vectors, we transfected shFoxp4-1, shFoxp4-2, or shFoxp4-sc with pCAGGS-GFP into the E14.5 cortex by IUE. The inhibition of *Foxp4* was assessed by immunofluorescence at E16.5. The ratio of FOXP4-positive cells in the transfected population was much less in the cortex receiving the interfering shRNAs than that of the scrambled shRNA (Fig. 2A and A′, percentage of GFP^+FOXP4^+ cells: shFoxp4-sc 66.29% *vs* shFoxp4-1 29.91% and shFoxp4-2 28.15%), showing that the shRNAs were able to repress *Foxp4* expression *in vivo*.

The E14.5-transfected brains were harvested at E17.5 to evaluate the location of *Foxp4* KD cells in the developing cerebral cortex. As expected, a large proportion of cells transfected with the control plasmid shFoxp4-sc crossed the IZ and reached the upper layer of the CP. By contrast, far fewer GFP^+ cells migrated to the CP in the KD groups (Fig. 2B and B′, percentage of cells in the CP: shFoxp4-sc 35.79% *vs* shFoxp4-1 13.90%, and shFoxp4-2 4.38%). The majority of cells with Foxp4 KD accumulated in the SVZ/VZ and failed to leave the IZ (Fig. 2B and B′, IZ: shFoxp4-sc 32.53% *vs* shFoxp4-1 48.61% and shFoxp4-2 51.90%; SVZ/VZ: shFoxp4-sc 31.68% *vs* shFoxp4-1 37.49% and shFoxp4-2 43.73%). To study if the abnormal location of cortical neurons is still present at a later stage, we examined the transfected brains at P3. In control brains, almost all electroporated GFP^+ cells had reached the upper layers of the CP (Fig. 2C and C′, percentage of cells in the CP: shFoxp4-sc 93.97%), showing completion of the radial migration. In contrast, only 72.14% and 57.76% of GFP^+ cells were detected in the superficial layer of the shFoxp4-1- and shFoxp4-2-transfected cortex, respectively. Many *Foxp4*-KD cells were still stalled and formed an ectopic nodule in the white matter (WM) (Fig. 2C). These data demonstrate that *Foxp4* expression is required for the proper positioning of cortical cells during embryonic development.

Knockdown of FOXP family member FOXP1 inhibits the radial migration of cortical neurons [14]. To exclude the possibility that *Foxp4* shRNA may mediate the KD from off-target effects, we analyzed the expression of the closely-related protein FOXP1 at P3 when the transfected cells co-localize with FOXP1 in the cortex. We examined the superficial cortical layers where all or part of E14.5-transfected cells resided at P3 (Fig. 2D). The fractions of $FOXP1^+$ cells in the transfected population were similar in the brains receiving shFoxp4-sc and shFoxp4-1 or shFoxp4-2 (Fig. 2D and D′, percentage of GFP^+FOXP1^+ cells in layers II–IV: shFoxp4-sc 82.51% *vs* shFoxp4-1 79.92 % and shFoxp4-2 84.07 %), supporting the conclusion that the shRNA acts specifically *in vivo*.

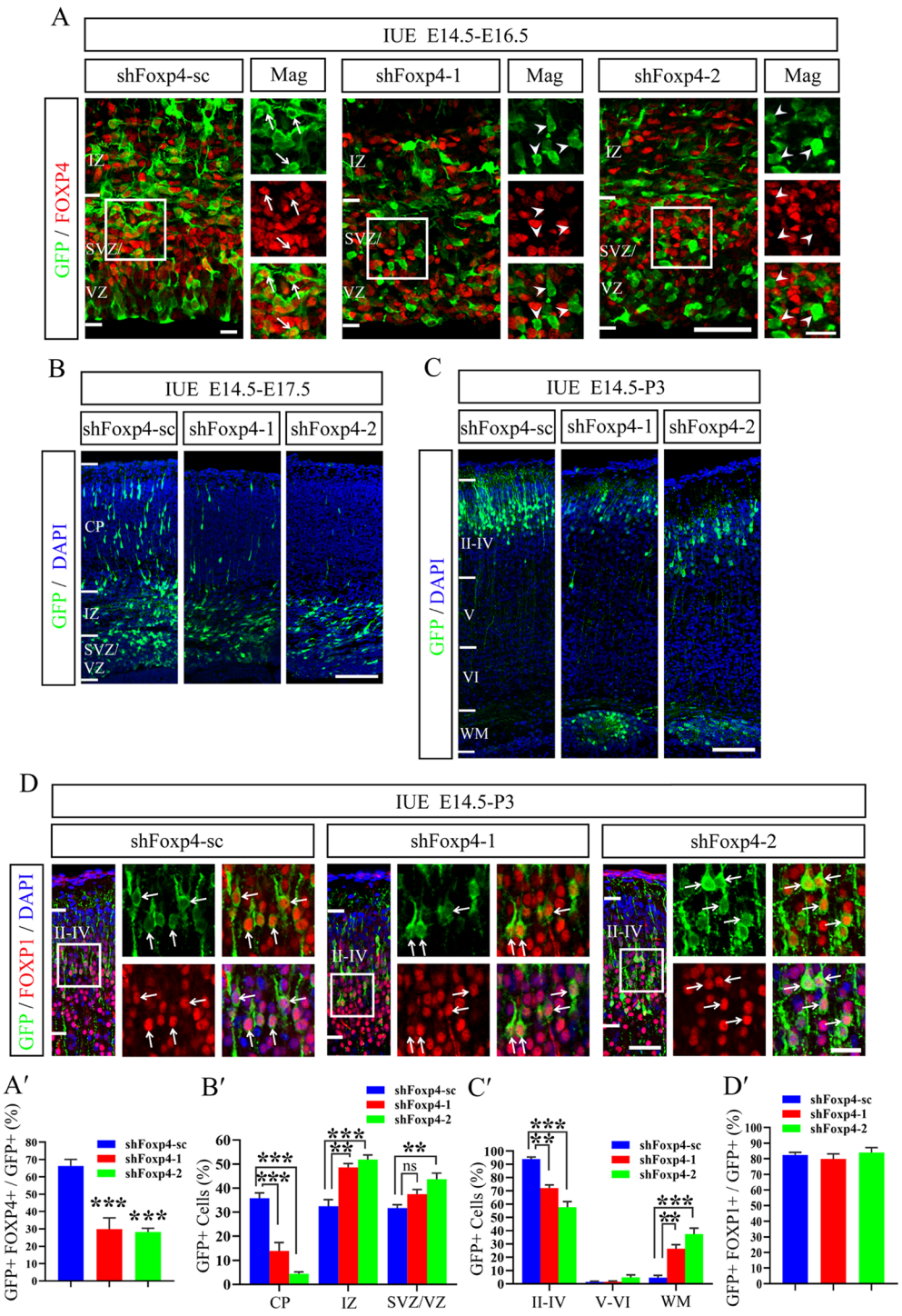

Fig. 2 Knocking down *Foxp4* alters the positioning of cortical cells. **A** Cortices at E16.5 immunostained with anti-FOXP4 (red) and GFP antibodies (shFoxp4-sc, shFoxp4-1, or shFoxp4-2 with pCAGGS-GFP was transfected into E14.5 cortices by IUE). Arrows indicate GFP$^+$ cells that express FOXP4 and arrowheads indicate those that do not. Scale bar, 50 μm (left panel) and 20 μm (right panels). **A′** Ratio of FOXP4$^+$ cells in the transfected population in **A** (shFoxp4-1 and shFoxp4-2 reduce the FOXP4$^+$ cells *in vivo*). n = 3–4 brains, ***P < 0.001, one-way analysis of variance (ANOVA), followed by Tukey's multiple-comparisons test. **B, C** E14.5-electroporated cortices at E17.5 (**B**) and P3 (**C**). Nuclei are counterstained with DAPI (blue). Scale bars, 50 μm. WM: white matter. **B′**, **C′** The distribution of GFP$^+$ cells in distinct cortical regions in **B** and **C**. n = 3–4 brains, ***P < 0.001, **P < 0.01. ns: no significant difference. **D** Brains receiving shRNAs immunostained with FOXP1 (red) and GFP antibodies at P3. Arrows mark the GFP$^+$ cells expressing FOXP1. Scale bar, 50 μm (left panel) and 20 μm (right panels). **D′** Ratios of GFP$^+$ cells co-expressing FOXP1 in layers II–IV. The *Foxp4*-interfering shRNAs did not change the expression of FOXP1.

Knockdown of *Foxp4* Alters the Proliferation and Differentiation of RGCs

To determine the identities of the ectopic cells after *Foxp4* KD, we immunostained brain sections with the cell-type-specific markers TBR2 and SATB2 (a marker for immature neurons). *Foxp4* inhibition decreased the proportion of GFP^+SATB2^+ cells in the CP compared to the control (Fig. 3A and C, percentage of GFP^+SATB2^+ cells in the CP: shFoxp4-sc 35.01% *vs* shFoxp4-2 5.58%), confirming the deficiency in neuronal migration. We also noted that KD of *Foxp4* led to the ectopic spill-over of GFP^+SATB2^+ neurons to the SVZ/VZ, in contrast to the control brain where $SATB2^+$ cells were excluded from the SVZ/VZ (Fig. 3A and C, percentage of GFP^+SATB2^+ cells in the SVZ/VZ: shFoxp4-sc 0% *vs* shFoxp4-2 14.88%). TBR2-labeled GFP^+ cells normally resided in the SVZ but not the apical surface of the VZ as expected for basal progenitor cells. However, in the shFoxp4-2-transfected brain, TBR2-positive cells were found in the apical VZ, in addition to being present in the VZ/SVZ (non-apical VZ) (Fig. 3B and D, percentage of GFP^+TBR2^+ cells at the apical VZ: shFoxp4-sc 0 % *vs* shFoxp4-2 5.53%). The VZ is the neurogenic layer of epithelial cells that lines the neural tube during the development of the cerebral cortex. The proliferation of neural progenitor cells is sustained in the VZ, which consists almost exclusively of dividing precursors. When neural precursors are removed from the VZ, they exit the cell cycle and differentiate, suggesting that the VZ provides a supportive environment for proliferation [32]. The ectopic location of $TBR2^+$ basal progenitor cells and $SATB2^+$ neurons in the VZ indicates a possible loss of the cellular microenvironment required for supporting the self-renewal of neural stem cells.

To investigate whether precocious differentiation in the VZ may be associated with changes in the proliferation of RGCs, we applied pH3 (an M-phase marker) immunostaining to the electroporated brain. We noted that KD induced a distinct localization of mitotic cells. Most of the GFP^+pH3^+ cells were normally aligned on the ventricle wall in the control brains. By contrast, upon *Foxp4* KD, the mitotic GFP^+pH3^+ cells were no longer concentrated on the apical surface of the VZ (Fig. 3E, F, percentage of GFP^+pH3^+ cells at the apical VZ: shFoxp4-sc 5.34% *vs* shFoxp4-2 1.06%), but were ectopically scattered across the VZ/SVZ, and occasionally in the IZ (non-apical VZ) (Fig. 3E, F, percentage of GFP^+pH3^+ cells at the non-apical VZ: shFoxp4-sc 1.67% *vs* shFoxp4-2 6.20%). Thus, the proliferating cells had detached from the neuroepithelium and abnormally intermingled with basal progenitor cells and neurons, suggesting that KD of *Foxp4* disrupts the lamination of the developing cortex.

Foxp4 KD Disrupts the Polarity of RGCs and the Integrity of the Neuroepithelium

Proper interactions between neural precursor cells generate a supportive niche to regulate self-renewal in the VZ [24]. To explore whether the aberrant proliferation and differentiation of RGCs were caused by the alteration of cell-cell contacts, we examined the morphology of RGCs and the integrity of the neuroepithelium in the VZ by nestin immunofluorescence. Nestin is an intermediate filament protein participating in the regulation of cell shape and mechanical integrity [33]. E14.5 embryos were electroporated with either shFoxp4-2 or the control plasmid and analyzed at E17.5. RGCs in the control group had bipolar morphology with dense and well-arranged fibers perpendicular to the pial surface. The VZ neuroepithelium contained uniformly packed RGCs, the apical processes of which formed an end-foot attachment connecting the cell body to the ventricular lumen. In contrast, the RGCs transfected with shFoxp4-2 were disorganized, and the apical surface was irregularly bent (Fig. 4A), suggesting that *Foxp4* KD disrupts the integrity of the neuroepithelium in the VZ.

As the RGCs with *Foxp4* KD looked disoriented, we examined the polarity of RGCs by γ-tubulin staining of centrosomes. Centrosomes anchor to the apical surface and control the mechanical properties of RGCs [34]. In control brains, centrosomes were positioned at the apical surface of RGCs during the interphase of the cell cycle. Occasionally, two separated centrosomes were spotted on opposite sides of a dividing nucleus (Fig. 4B). However, the KD of *Foxp4* caused γ-tubulin positive puncta to scatter randomly throughout the VZ, with reduced apical condensation (Fig. 4B, C), supporting the conclusion that the KD disrupts the anchorage of centrosomes to the apical membrane and destroys the apico-basal polarity of the RGCs.

Foxp4 is Essential for the N-cadherin-dependent Adhesion of RGCs

The integrity of VZ neuroepithelium and the apico-basal polarity of RGCs are maintained by AJs that form adhesions between the adjacent progenitor cells [20, 35, 36]. N-cadherin and β-catenin are the AJ proteins in the neurogenic niche of the developing cerebral cortex [23]. We first examined the expression of N-cadherin in the developing cerebral cortex. N-cadherin was prominently concentrated in the apical end-feet of the RGCs throughout the development from E12.5 to P0. However, at higher magnification, subtle differences became notable. At early time points (E12.5 and E14.5), N-cadherin staining produced a continuous solid band lining the luminal surface of the ventricle even at a higher magnitude. In contrast, the apical N-cadherin staining

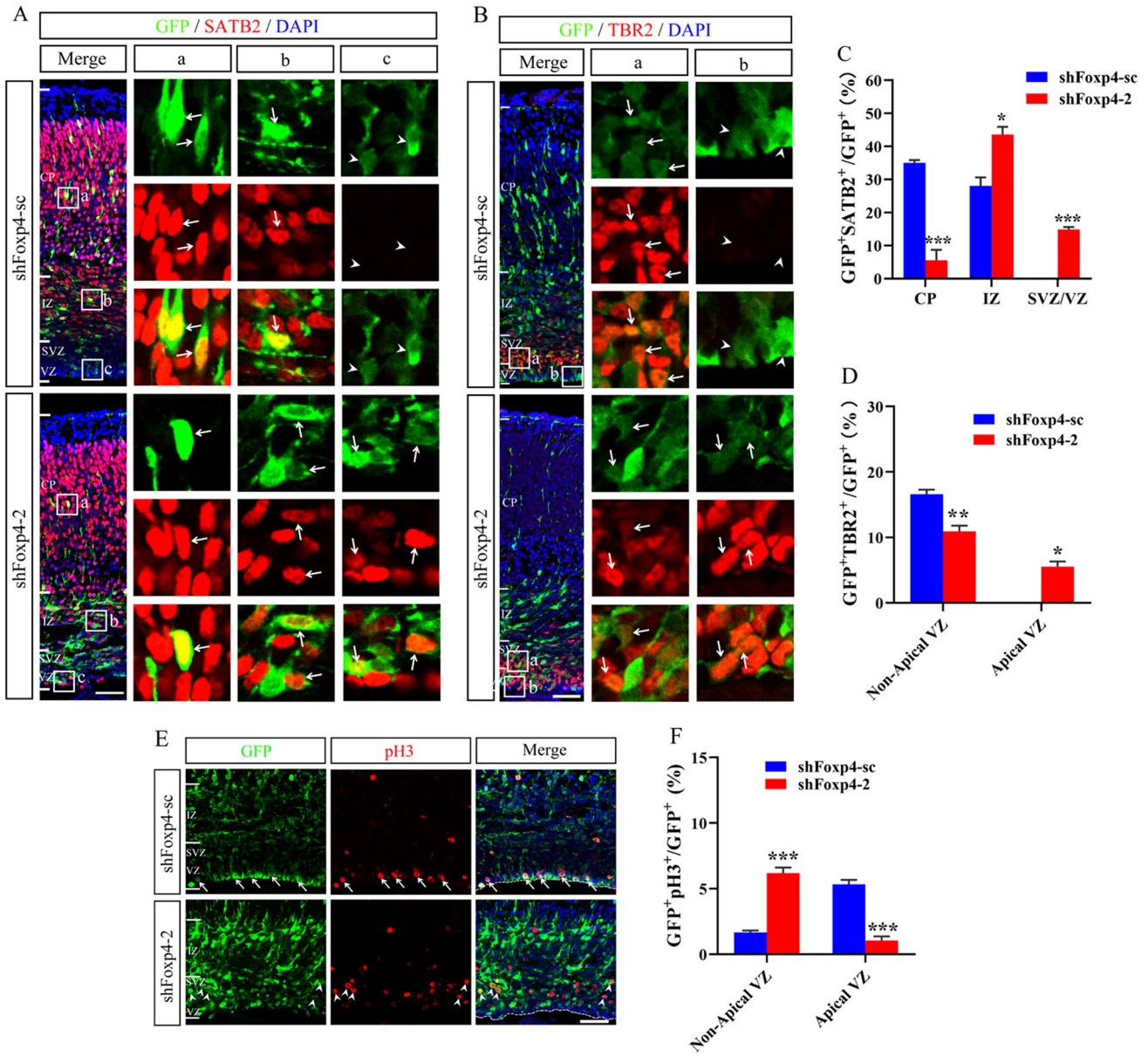

Fig. 3 Knockdown of *Foxp4* induces the ectopic proliferation and differentiation of RGCs. **A** Coronal sections immunostained with GFP and SATB2 (red) antibodies at E17.5 (pCAGGS-GFP plus either shFoxp4-sc or shFoxp4-2 were co-transfected into E14.5 mouse brains). Nuclei are counterstained with DAPI (blue). (**a-c**) Magnified images of transfected cells in the CP (**a**), IZ (**b**), and SVZ/VZ (**c**). Arrows indicate the GFP^+ cells expressing SATB2 and arrowheads indicate those that do not. Scale bars, 50 μm (left panel) and 10 μm (right panels). **B** Brain sections stained with TBR2 (red) and GFP antibodies; nuclei are counterstained with DAPI (blue). (**a**, **b**) Magnified images of boxes showing transfected cells in the non-apical (**a**) and apical VZ (**b**). Arrows indicate GFP^+ cells expressing TBR2 and arrowheads indicate those that do not. Scale bars 50 μm (left panel) and 10 μm (right panels). **C**, **D** Quantification of the GFP^+ cells co-expressing SATB2 (**C**) or TBR2 (**D**) in the indicated regions. $n = 3$ brains, $^{***}P < 0.001$, $^{**}P < 0.01$, $^{*}P < 0.05$, *t*-test. **E** Representative images of E17.5 brain sections immunostained for pH3 (red). Arrows indicate the $pH3^+GFP^+$ progenitors confined to the apical surface of the VZ. Arrowheads mark the $pH3^+GFP^+$ cells in the non-apical VZ. Scale bars, 50 μm. **F** Proportions of $pH3^+GFP^+$ cells in the apical and non-apical VZ. $n = 3$, $^{***}P < 0.001$, *t*-test.

appeared weaker and irregular at E16.5 and intermittently disappeared at P0, although honeycomb-like staining of N-cadherin mediating the side contacts was nevertheless present in the VZ (Fig. 5A). The results suggest that the luminal clustering of N-cadherin in the RGCs is reduced or interrupted during late cortical neurogenesis.

To determine whether disorganization of the cortical lamina is related to the loss of N-cadherin-based AJs,

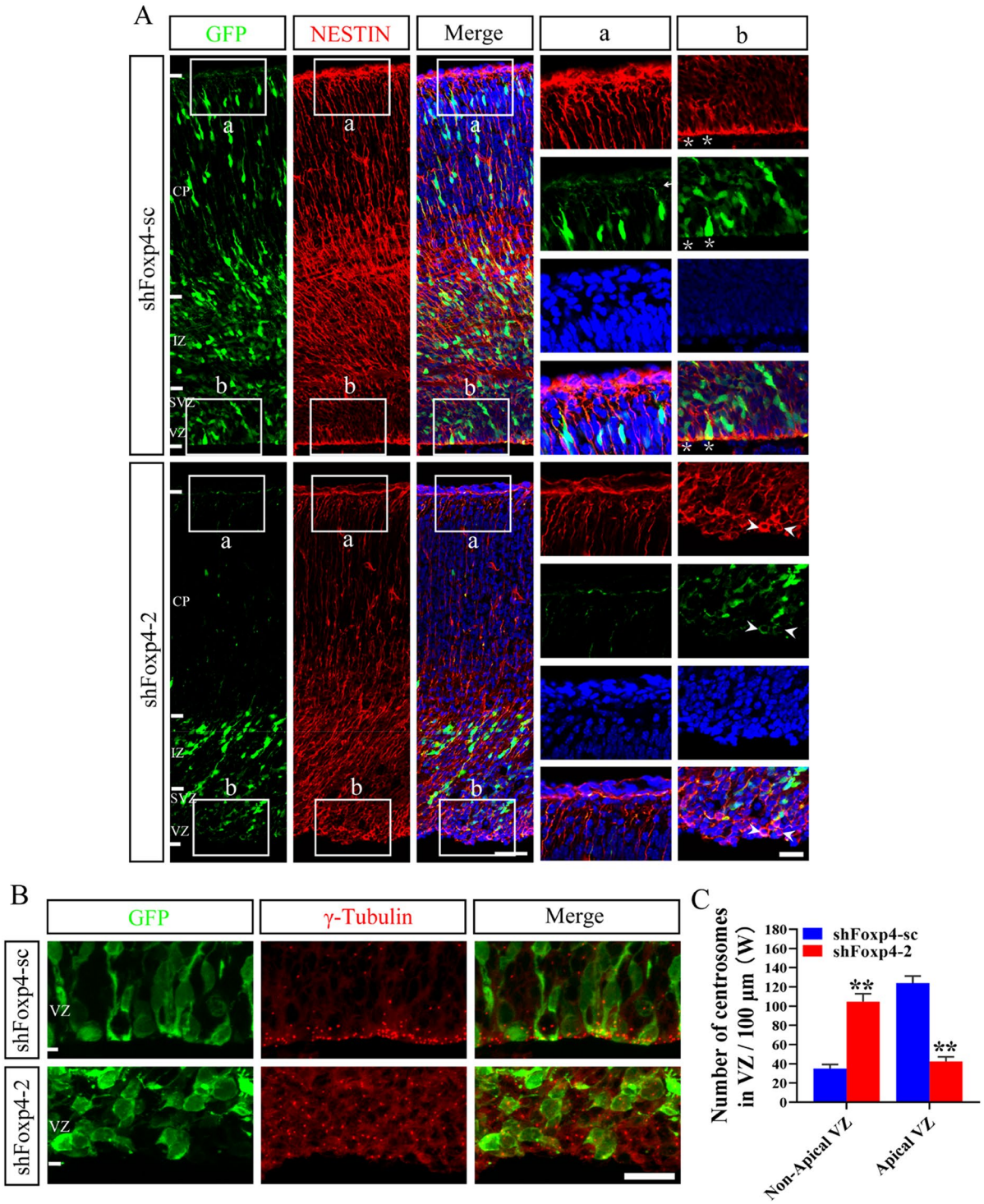

Fig. 4 Suppression of *Foxp4* disrupts the integrity of neuroepithelium and the polarity of RCGs. **A** Cortical sections were stained for NESTIN (red) and GFP at E17.5 (shFoxp4-sc or shFoxp4-2, along with pCAGGS-GFP, were delivered into RGCs of the E14.5 mouse cortex). **a**, **b** Magnified views of the boxes in the left panel. shFoxp4-sc-transfected cells at the ventricular surface have apical end-feet attachment (asterisks). The cells expressing shFoxp4-2 show irregular shapes with diminished nestin in the apical region (arrowheads). Nuclei are stained with DAPI. Scale bars, 50 μm (left panels) and 20 μm (right panels). **B** Cortical sections immunostained with γ-tubulin (red) and GFP. γ-Tubulin is clustered in the luminal surface of the VZ in control, whereas in the KD brain, they are dispersed throughout the VZ. Scale bar, 20 μm. **C** Statistics of γ-tubulin-positive puncta (centrosomes) in the apical and non-apical surfaces of the VZ. $n = 3$ brains, $^{**}P < 0.01$, *t*-test.

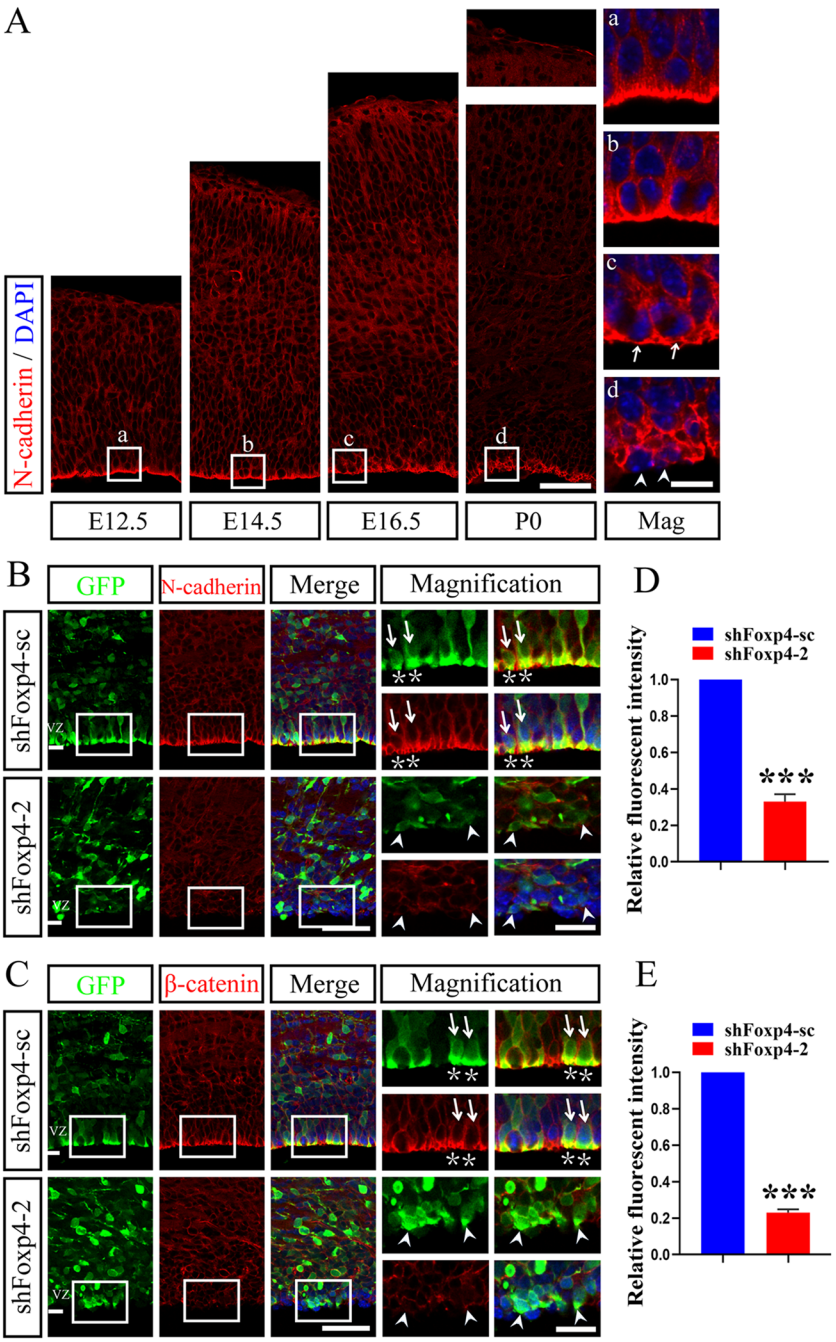

Fig. 5 Knockdown of *Foxp4* disrupts N-cadherin-based AJs in the VZ. **A** N-cadherin (red) expression pattern in mouse cortex on E12.5, E14.5, E16.5, and P0. **a–d** Magnification of selected luminal surfaces (boxes) in the left panel. Arrows indicate cells with thinner or weakened apical N-cadherin staining. Arrowheads illustrates the loss of N-cadherin expression on the apical surface. Scale bars, 50 μm (left panels) and 10 μm (right panels). **B, C** Representative images of N-cadherin (**B**) and β-catenin (**C**) immunostaining at E17.5 (pCAGGS-GFP plus either shFoxp4-sc or shFoxp4-2 was co-transfected into E14.5 mouse brains). Nuclei are stained with DAPI in the merged images. The right panels are magnified images from the boxes. Scale bars, 50 μm (left panels) and 20 μm (right panels). shFoxp4-sc-transfected cells display condensed N-cadherin (red) and β-catenin (red) expression at the ventricular surface (arrows and asterisks). The *Foxp4* KD cells lack apical clustering of N-cadherin or β-catenin (arrowheads). **D, E** Fluorescence intensity of N-cadherin (**B**) and β-catenin (**C**) along the VZ surface of the transfected region as calculated by ImageJ, $n = 3$ brains, $^{***}P < 0.001$, paired *t*-test.

we examined N-cadherin and β-catenin in the brains with *Foxp4* KD. Immunostaining results showed that N-cadherin was intensely condensed on the VZ surface in the control brains. In contrast, in shFoxp4-2 transfected brains, the ventricular surface was largely devoid of the clustering of N-cadherin (Fig. 5B, D), suggesting that the KD of *Foxp4* likely dissolved the N-cadherin-based AJs. β-catenin is the intracellular binding partner for N-cadherin, and the binding stabilizes the cadherin zipper structure in AJs [37]. The intensity of β-catenin staining in the apical end-feet was severely reduced in shFoxp4-2-transfected brains compared to the control (Fig. 5C, E). These results indicate that *Foxp4* KD represses the accumulation of the AJ protein N-cadherin and β-catenin in the apical processes of RGCs, suggesting disruption of N-cadherin-based AJs by KD.

Since N-cadherin is essential for radial migration [20] and AJs maintain the self-renewal of the neural progenitors in the VZ [24, 38], we postulated that the defective migration and ectopic differentiation induced by the KD might be caused by the loss of N-cadherin clustering. To test this, we introduced

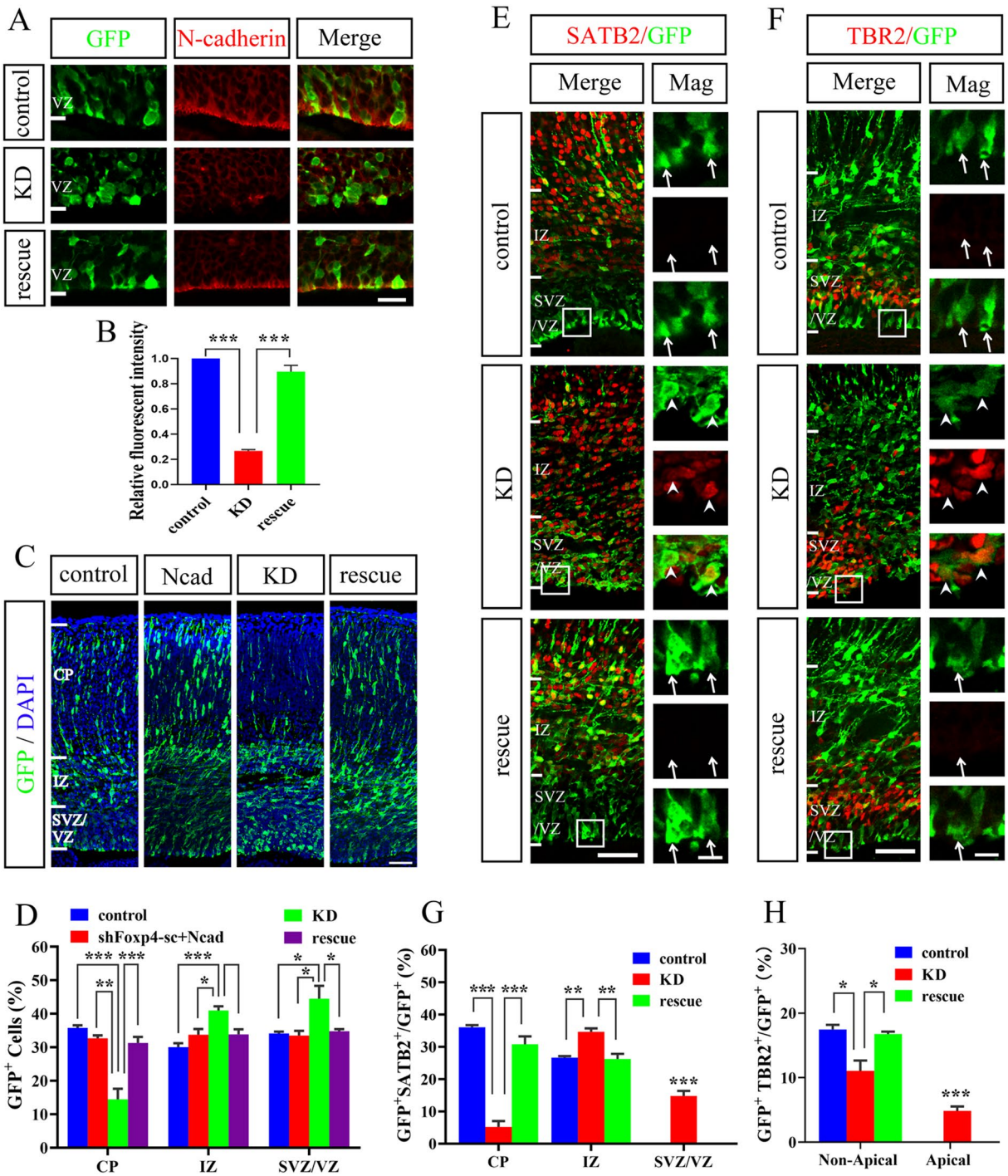

Fig. 6 Expression of N-cadherin restores radial migration and neuronal differentiation. **A** E14.5 cortices transfected with shFoxp4-sc plus pCAGEN (control), shFoxp4-2 plus pCAGEN (KD), or shFoxp4-2 plus pCAG-Ncad (rescue) immunostained for N-cadherin (Red) at E17.5. The rescue partially recovered the apical condensation of N-cadherin. Scale bar, 20 μm. **B** Relative fluorescence intensity of N-cadherin (**A**) at the ventricular surface. n = 3 brains, ***P <0.001, paired t-test. **C** Distribution of GFP-labeled cells in the E17.5 cortex electroporated with indicated plasmids at E14.5. Scale bar, 50 μm. **D** Proportions of GFP$^+$ cells in distinct cortical regions as calculated from **C**. Expression of *N-cadherin* restored the cells migrating toward the CP. n = 3, ***P <0.001, **P <0.01, *P <0.05, one-way ANOVA. **E, F** Representative images of SATB2 (**E**) and TBR2 (**F**) immunostaining in the E17.5 cortex. Arrows indicate that the electroporated cells on the apical surface do not express SATB2 (red) or TBR2 (red). Arrowheads show the presence of GFP$^+$SATB2$^+$ or GFP$^+$TBR2$^+$ cells at the ventricular surface. Scale bars, 50 μm (left images) and 10 μm (right images). **G, H** Quantification of the GFP$^+$ cells co-expressing SATB2 in the indicated lamina (**E**) and TBR2 in the non-apical and apical VZ (**F**). n = 3 brains, ***P <0.001, **P <0.01, *P <0.05, t-test.

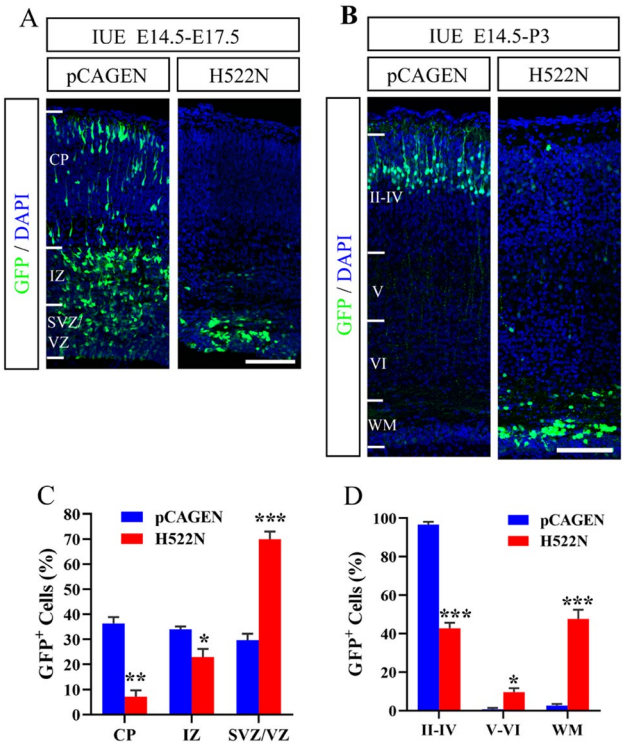

Fig. 7 Expression of the *Foxp4* mutant leads to periventricular heterotopia. **A, B** E14.5 embryos were electroporated with pCAGEN or mFoxp4-H522N in the presence of pCAGGS-GFP. The brains were harvested and sectioned at E17.5 (**A**) or P3 (**B**). Scale bars, 50 μm. **C, D** Fractions of GFP^+ cells in each cortical layer as calculated from **A** and **B**. $n = 3$, $^{***}P < 0.001$, $^{**}P < 0.01$, $^{*}P < 0.05$, *t*-test.

shFoxp4-2, in the presence or absence of the *N-cadherin* expression construct (pCAG-Ncad), into the RGCs at E14.5. The brains were sectioned and analyzed at E17.5. Expression of WT *N-cadherin* in *Foxp4*-KD brains recovered the N-cadherin-positive belt facing the ventricle (Fig. 6A, B). Overexpression of *N-cadherin* substantially up-regulated the population of cells migrating into the CP compared to that expressing shFoxp4-2 alone (Fig. 6C, D, CP: shFoxp4-sc + pCAGEN: 35.79%, shFoxp4-sc + pCAG-Ncad: 32.71%, shFoxp4-2 + pCAGEN: 14.48%, shFoxp4-2 + pCAG-Ncad: 31.31%). Mis-expression of *N-cadherin* alone did not disturb the normal radial migration (Fig. 6C, D). The ectopic distribution of $SATB2^+$ or $TBR2^+$ cells in the apical surface of the VZ caused by the *Foxp4* KD disappeared upon the introduction of *N-cadherin* (Fig. 6E–H). The rescue experiment supports the conclusion that KD of *Foxp4* inhibits neuronal migration and alters the differentiation of RGCs by regulating *N-cadherin*.

Expression of a *Foxp4* Mutant Leads to Periventricular Heterotopia

The genetic mutation of *FOXP4* is linked to severe neurodevelopmental disorders with speech/language delays, growth defects, and variable congenital abnormalities. The heterozygous *de novo* mutation H517N located in the foxhead box DNA-binding domain of *FOXP4* has been reported in a child with delayed speech development and intellectual disability [10]. The mutant shows a loss of the transcriptional repression capability but has an intact leucine zipper motif that mediates the interaction with FOXP4 protein. A study with bioluminescence resonance energy transfer confirmed that the mutant is able to dimerize with WT FOXP4 [10]. To elucidate the relationship between the *FOXP4* heterozygous mutation and the neuropathology, we created mFoxp4-H522N, a mouse homolog of the human variant H517N. We introduced mFoxp4-H522N and pCAGGS-GFP into the E14.5 mouse neocortex, which was analyzed at E17.5 and P3. Similar to *Foxp4*-KD, the mutant-transfected cells failed to migrate to the CP (Fig. 7A, C, percentage of cells in CP: pCAGEN 32.35% *vs* mFoxp4-H522N 7.10%) but stalled in the SVZ/VZ at E17.5 (Fig. 7A, C, percentage of cells in the SVZ/VZ: pCAGEN 29.70% *vs* mFoxp4-H522N 69.98%). At P3, GFP^+ cells formed an ectopic nodule in the WM (Fig. 7B, D, percentage of cells in the WM: pCAGEN 2.58% *vs* mFoxp4-H522N 47.61%). In comparison, the majority of vector-transfected neurons were normally settled in the superficial layers (Fig. 7B, D, percentage of cells in layers II–IV: pCAGE: 96.69% *vs* mFoxp4-H522N 42.80%). These data suggest that the mis-expression of H522N results in abnormal positioning of cortical cells and periventricular heterotopia.

To investigate the impact of the loss-of-function *Foxp4* variant on RGC differentiation, we immunostained the brain sections using TBR2 and SATB2 antibodies at E17.5. The percentage of $SATB2^+$ newborn neurons in the SVZ/VZ increased in the mutant-electroporated cortices compared with the control (Fig. 8A, C, percentage of GFP^+SATB2^+ cells in the SVZ/VZ: pCAGEN 0% *vs* mFoxp4-H522N 12.86%). Furthermore, the mutant led to $TBR2^+$ cells on the apical surface of the VZ (Fig. 8B, D, percentage of GFP^+TBR2^+ cells at the apical VZ: pCAGEN 0% *vs* mFoxp4-H522N 6.24%). These ectopic phenotypes were similar to those induced by *Foxp4* shRNAs (Fig. 3). To determine whether the precocious locations were related to the alteration of N-cadherin, we examined the expression of *N-cadherin*. The cortices expressing the control vector had intense N-cadherin staining lining the luminal surface of the VZ. However, overexpression of mFoxp4-H522N diminished the apical clustering of N-cadherin (Fig. 8E, F). This finding indicates that the overexpression of H522N probably disrupts the N-cadherin-based AJs and leads to the abnormal differentiation of RGCs.

Discussion

Genetic loss-of-function mutations of *FOXP4* have been implicated in cognitive disorders that affect language

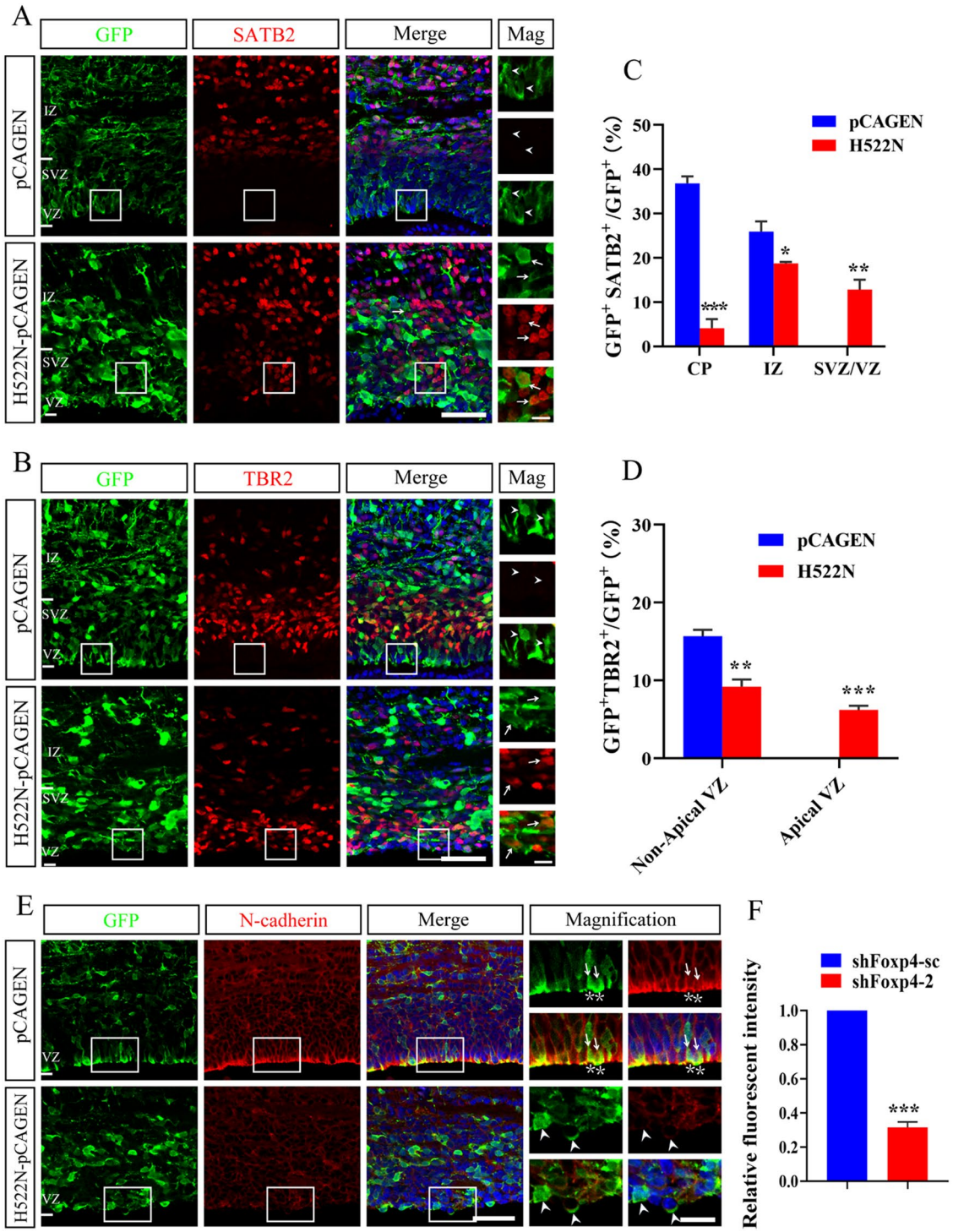

Fig. 8 mFoxp4-H522N induces ectopic differentiation of RGCs and reduces apical N-cadherin. **A, B** Brain sections immunostained for SATB2 (red, **A**) or TBR2 (red, **B**) at E17.5 (E14.5 cortices were transfected with pCAGEN or mFoxp4-H522N in the presence of pCAGGS-GFP). Nuclei are stained with DAPI. The right panels are magnified images of the boxes in VZ/SVZ (**A**) or apical VZ (**B**). Arrowheads indicate that the transfected cells do not express SATB2 (**A**) or TBR2 (**B**). Arrows designate co-localization of the cell type maker with GFP. Scale bars, 50 μm (left images) and 10 μm (right images). **C, D** Proportions of $SATB2^+GFP^+$ (**C**) or $TBR2^+GFP^+$ (**D**) cells in the specified regions. n = 3, $^{***}P$ <0.001, $^{**}P$ <0.01, $^{*}P$ <0.05, t-test. **E** Co-staining of N-cadherin (red) and GFP in the E17.5 mouse brain. Nuclei are stained with DAPI. Control plasmid-transfected cells have intense N-cadherin at the ventricular surface (arrows and asterisks). mFoxp4-H522N-expressing cells are devoid of the clustering of N-cadherin (arrowheads). Scale bars, 50 μm (left images) and 20 μm (right images). **F** Relative fluorescent intensity of N-cadherin (**E**) at the ventricular surface. n = 3 brains, $^{***}P$ <0.001, paired t-test.

acquisition and intellectual development. In this study, we found that the transcription factor FOXP4 was expressed in RGCs (Fig. 1B). Interestingly, the transmembrane protein N-cadherin formed prominent end-feet in the apical surface of the RCGs during the early stage of cortical neurogenesis. The end-feet became less compact and disappeared sporadically at birth (Fig. 5A). The N-cadherin in RGCs appears to be regulated by *Foxp4* as both knockdown and dominant-negative inhibition of *Foxp4* by IUE led to the loss of its surface condensation (Figs 5B and 8E). Although *in utero* electroporation transfected only a small subset of cortical cells, the disruption of surface N-cadherin along the VZ and the orientation of RGCs across the infected region seemed to be global (Fig. 5). This discrepancy is puzzling but has been noted in previous studies on AJs by IUE, and explained by the postulation of non-cell-autonomous actions across the neuroepithelium [39, 40].

Foxp4 KD disrupted N-cadherin-based AJs and the integrity of the VZ neuroepithelium, leading to ectopic neurogenesis (Fig. 3). The inhibition of *Foxp4* also eliminated the apico-basal polarity of RGCs (Fig. 4), and rendered the RGCs unable to support radial migration (Fig. 2B). The faulty position of cortical neurons may also arise directly from the lack of cadherin-based adhesion since the attachment of migrating neurons to the radial glial fibers depends on homophilic interactions between N-cadherin proteins located in the RGC and the neuron [20, 41]. Overexpressing N-cadherin reversed the ectopic differentiation and deficient migration, indicating that *Foxp4* mediates the KD effects by regulating N-cadherin.

Foxp4 and *Foxp2* are expressed in the spinal cord during motor neuron development. A graded increase in the expression of *Foxp4* coincides with the downregulation of N-cadherin and detachment of neural progenitor cells from the neuroepithelium. Mis-expressing either *Foxp4* or *Foxp2* represses the expression of N-cadherin *in vivo* [26]. The apparent conflicting results in the regulation of *N-cadherin* by *Foxp4* between the developing cerebral cortex and the spinal cord might be related to spatial differences in the neuroepithelia. However, we noted that the expression of N-cadherin in the neuroepithelium is reduced in the developing spinal cord of the *Foxp4* knockout mice, as shown in the same study that demonstrates the inhibition of N-cadherin by mis-expressing *Foxp4*. The *Foxp4* knockout mice also exhibited disruption of the neuroepithelial cytoarchitecture ([26]: supplemental Fig. S8 panels T and Y). Thus, we do not exclude the possibility that N-cadherin and the integrity of neuroepithelia may be under dual regulation of the transcription factor FOXP4.

The molecular and cellular mechanisms responsible for the regulation of *N-cadherin* by *Foxp4* are unclear. *N-cadherin* may be a direct target of *Foxp4*, which binds to a highly conserved element within intron 3 of *N-cadherin* [26], although we do not know if this binding site contributes to the positive or negative regulation of *N-cadherin* expression. Alternatively, *Foxp4* may control *N-cadherin* indirectly in the plasma membrane. After biosynthesis from the Golgi complex, N-cadherin density at the AJs is regulated by recycling between internal and plasma membrane pools [42]. N-cadherin in the plasma membrane undergoes rapid internalization that is required for synaptic plasticity [43]. It remains to be determined whether *Foxp4* regulates the endocytic machinery in neural progenitors. However, FOXP subfamily member FOXP1 represses the expression of huntingtin-interacting protein 1-related, which controls the internalization of cell surface receptors *via* endocytosis in the germinal center of diffusive large B-cell lymphoma [44]. Furthermore, the stability of cadherin-based AJs is controlled by protein tyrosine phosphorylation of associated components in the cell adhesion complex [45]. For example, phosphorylation of the binding partner β-catenin on tyrosine residue 654 modulates endocytosis by enhancing its association with N-cadherin, and over-expression of the tyrosine mutant Y654F promotes the surface population of N-cadherin [43]. Interestingly, FOXP4 promotes β-catenin transcription by binding to the β-catenin promoter in esophageal squamous cell carcinoma [46]. Future studies are needed to explore the molecular mechanisms underlying the regulation of N-cadherin-based AJs by *Foxp4*.

In human patients, most heterozygous mutations of *FOXP4* cause a loss-of-function in the mutated protein [10], leading to the haploinsufficiency of this transcription factor. However, as the mutants remain able to interact with WT FOXP4, the mutated protein may further interfere with the normal function of the WT allele *via* dimerization. Since Foxp4-H522N repressed the apical clustering of N-cadherin, induced the ectopic differentiation of RGCs, and impeded radial migration in the mouse brain that harbored two WT alleles of *Foxp4* (Figs 7 and 8), the abnormalities found in the mFoxp4-H522N-expressing brains cannot be attributed to loss of the WT FOXP4 protein. Instead, the function of WT *Foxp4* was likely compromised by the introduced mutant. Therefore, human heterozygous mutants may exacerbate the severity of NDDs by superimposing their interference on that from a heterozygous loss of *FOXP4*.

In conclusion, in this study, we found that the loss of *Foxp4* induces ectopic neurogenesis and inhibits radial migration by disrupting N-cadherin-based AJs in the germinal zone. Deficiency in migration and periventricular heterotopias are hallmarks of human neurological and psychiatric disorders [18, 27, 47]. The malformation of the cerebral cortex may underlie the NDDs associated with the *FOXP4* mutations, supporting a causal relationship between loss-of-function *FOXP4* variants and NDDs in humans.

Acknowledgements This work was supported by the Wenzhou Municipal Science and Technology Bureau (Y20210901), the Natural Science Foundation of Zhejiang Province (LQ20H090001), and the Scientific Research Fund of Wenling Science and Technology Bureau (2018C320001).

Conflict of interest The authors have no competing financial interests to declare.

References

1. Teufel A, Wong EA, Mukhopadhyay M, Malik N, Westphal H. FoxP4, a novel forkhead transcription factor. Biochim Biophys Acta 2003, 1627: 147–152.
2. Bowers JM, Konopka G. The role of the FOXP family of transcription factors in ASD. Dis Markers 2012, 33: 251–260.
3. Lai CSL, Fisher SE, Hurst JA, Vargha-Khadem F, Monaco AP. A forkhead-domain gene is mutated in a severe speech and language disorder. Nature 2001, 413: 519–523.
4. Morgan AT, Webster R. Aetiology of childhood apraxia of speech: A clinical practice update for paediatricians. J Paediatr Child Health 2018, 54: 1090–1095.
5. Hamdan FF, Daoud H, Rochefort D, Piton A, Gauthier J, Langlois M. *De novo* mutations in *FOXP1* in cases with intellectual disability, autism, and language impairment. Am J Hum Genet 2010, 87: 671–678.
6. O'Roak BJ, Deriziotis P, Lee C, Vives L, Schwartz JJ, Girirajan S, *et al*. Exome sequencing in sporadic autism spectrum disorders identifies severe *de novo* mutations. Nat Genet 2011, 43: 585–589.
7. Sollis E, Graham SA, Vino A, Froehlich H, Vreeburg M, Dimitropoulou D, *et al*. Identification and functional characterization of *de novo* FOXP1 variants provides novel insights into the etiology of neurodevelopmental disorder. Hum Mol Genet 2015, 25: 546–557.
8. Medvedeva VP, Rieger MA, Vieth B, Mombereau C, Ziegenhain C, Ghosh T, *et al*. Altered social behavior in mice carrying a cortical Foxp2 deletion. Hum Mol Genet 2018, 28: 701–717.
9. Bacon C, Schneider M, Le Magueresse C, Froehlich H, Sticht C, Gluch C, *et al*. Brain-specific Foxp1 deletion impairs neuronal development and causes autistic-like behaviour. Mol Psychiatry 2015, 20: 632–639.
10. Snijders Blok L, Vino A, den Hoed J, Underhill HR, Monteil D, Li H, *et al*. Heterozygous variants that disturb the transcriptional repressor activity of *FOXP4* cause a developmental disorder with speech/language delays and multiple congenital abnormalities. Genet Med 2021, 23: 534–542.
11. Noctor SC, Martínez-Cerdeño V, Ivic L, Kriegstein AR. Cortical neurons arise in symmetric and asymmetric division zones and migrate through specific phases. Nat Neurosci 2004, 7: 136–144.
12. Nadarajah B, Parnavelas JG. Modes of neuronal migration in the developing cerebral cortex. Nat Rev Neurosci 2002, 3: 423–432.
13. Kwan KY, Sestan N, Anton ES. Transcriptional co-regulation of neuronal migration and laminar identity in the neocortex. Development 2012, 139: 1535–1546.
14. Li X, Xiao J, Fröhlich H, Tu X, Li L, Xu Y, *et al*. Foxp1 regulates cortical radial migration and neuronal morphogenesis in developing cerebral cortex. PLoS One 2015, 10: e0127671.
15. Pearson CA, Moore DM, Tucker HO, Dekker JD, Hu H, Miquelajauregui A, *et al*. Foxp1 regulates neural stem cell self-renewal and bias toward deep layer cortical fates. Cell Rep 2020, 30: 1964-1981. e3.
16. Tsui D, Vessey JP, Tomita H, Kaplan DR, Miller FD. FoxP2 regulates neurogenesis during embryonic cortical development. J Neurosci 2013, 33: 244–258.
17. Garcia-Calero E, Botella-Lopez A, Bahamonde O, Perez-Balaguer A, Martinez S. FoxP2 protein levels regulate cell morphology changes and migration patterns in the vertebrate developing telencephalon. Brain Struct Funct 2016, 221: 2905–2917.
18. Buchsbaum IY, Cappello S. Neuronal migration in the CNS during development and disease: Insights from *in vivo* and *in vitro* models. Development 2019, 146: dev163766.
19. Kriegstein A, Alvarez-Buylla A. The glial nature of embryonic and adult neural stem cells. Annu Rev Neurosci 2009, 32: 149–184.
20. Shikanai M, Nakajima K, Kawauchi T. N-Cadherin regulates radial glial fiber-dependent migration of cortical locomoting neurons. Commun Integr Biol 2011, 4: 326–330.
21. Meng W, Takeichi M. Adherens junction: Molecular architecture and regulation. Cold Spring Harb Perspect Biol 2009, 1: a002899.
22. Miyamoto Y, Sakane F, Hashimoto K. N-cadherin-based adherens junction regulates the maintenance, proliferation, and differentiation of neural progenitor cells during development. Cell Adhesion Migr 2015, 9: 183–192.
23. Veeraval L, O'Leary CJ, Cooper HM. Adherens junctions: Guardians of cortical development. Front Cell Dev Biol 2020, 8: 6.
24. Zhang J, Woodhead GJ, Swaminathan SK, Noles SR, McQuinn ER, Pisarek AJ, *et al*. Cortical neural precursors inhibit their own differentiation via N-cadherin maintenance of beta-catenin signaling. Dev Cell 2010, 18: 472–479.
25. Farkas LM. The cell biology of neural stem and progenitor cells and its significance for their proliferation versus differentiation during mammalian brain development. Curr Opin Cell Biol 2008, 20: 707–715.
26. Rousso DL, Pearson CA, Gaber ZB, Miquelajauregui A, Li S, Portera-Cailliau C, *et al*. Foxp-mediated suppression of N-cadherin regulates neuroepithelial character and progenitor maintenance in the CNS. Neuron 2012, 74: 314–330.
27. Sheen VL, Basel-Vanagaite L, Goodman JR, Scheffer IE, Bodell A, Ganesh VS, *et al*. Etiological heterogeneity of familial periventricular heterotopia and hydrocephalus. Brain Dev 2004, 26: 326–334.
28. Sheen VL, Ganesh VS, Topcu M, Sebire G, Bodell A, Hill RS, *et al*. Mutations in $ARFGEF_2$ implicate vesicle trafficking in neural progenitor proliferation and migration in the human cerebral cortex. Nat Genet 2004, 36: 69–76.
29. Fox JW, Lamperti ED, Ekşioğlu YZ, Hong SE, Feng Y, Graham DA, *et al*. Mutations in filamin 1 prevent migration of cerebral cortical neurons in human periventricular heterotopia. Neuron 1998, 21: 1315–1325.
30. Chen JG, Rasin MR, Kwan KY, Sestan N. Zfp312 is required for subcortical axonal projections and dendritic morphology of deep-layer pyramidal neurons of the cerebral cortex. Proc Natl Acad Sci U S A 2005, 102: 17792–17797.
31. Takahashi K, Liu FC, Hirokawa K, Takahashi H. Expression of Foxp4 in the developing and adult rat forebrain. J Neurosci Res 2008, 86: 3106–3116.
32. Temple S. The development of neural stem cells. Nature 2001, 414: 112–117.
33. Sanghvi-Shah R, Weber GF. Intermediate filaments at the junction of mechanotransduction, migration, and development. Front Cell Dev Biol 2017, 5: 81.
34. Shao W, Yang J, He M, Yu XY, Lee CH, Yang Z, *et al*. Centrosome anchoring regulates progenitor properties and cortical formation. Nature 2020, 580: 106–112.
35. Gärtner A, Fornasiero EF, Munck S, Vennekens K, Seuntjens E, Huttner WB, *et al*. N-cadherin specifies first asymmetry in developing neurons. EMBO J 2012, 31: 1893–1903.
36. Kawauchi T, Sekine K, Shikanai M, Chihama K, Tomita K, Kubo KI, *et al*. Rab GTPases-dependent endocytic pathways regulate neuronal migration and maturation through N-cadherin trafficking. Neuron 2010, 67: 588–602.

37. Huber AH, Stewart DB, Laurents DV, Nelson WJ, Weis WI. The cadherin cytoplasmic domain is unstructured in the absence of beta-catenin. A possible mechanism for regulating cadherin turnover. J Biol Chem 2001, 276: 12301–12309.
38. Mutch CA, Schulte JD, Olson E, Chenn A. Beta-catenin signaling negatively regulates intermediate progenitor population numbers in the developing cortex. PLoS One 2010, 5: e12376.
39. Wang J, Li T, Wang JL, Xu Z, Meng W, Wu QF. Talpid3-mediated centrosome integrity restrains neural progenitor delamination to sustain neurogenesis by stabilizing adherens junctions. Cell Rep 2020, 33: 108495.
40. Romero DM, Poirier K, Belvindrah R, Moutkine I, Houllier A, LeMoing AG, *et al*. Novel role of the synaptic scaffold protein Dlgap4 in ventricular surface integrity and neuronal migration during cortical development. Nat Commun 2022, 13: 2746.
41. Wei C, Sun M, Sun X, Meng H, Li Q, Gao K, *et al*. RhoGEF trio regulates radial migration of projection neurons *via* its distinct domains. Neurosci Bull 2022, 38: 249–262.
42. Linford A, Yoshimura SI, Bastos RN, Langemeyer L, Gerondopoulos A, Rigden DJ, *et al*. Rab14 and its exchange factor FAM116 link endocytic recycling and adherens junction stability in migrating cells. Dev Cell 2012, 22: 952–966.
43. Tai CY, Mysore SP, Chiu C, Schuman EM. Activity-regulated N-cadherin endocytosis. Neuron 2007, 54: 771–785.
44. Wong KK, Gascoyne DM, Brown PJ, Soilleux EJ, Snell C, Chen H, *et al*. Reciprocal expression of the endocytic protein HIP1R and its repressor FOXP1 predicts outcome in R-CHOP-treated diffuse large B-cell lymphoma patients. Leukemia 2014, 28: 362–372.
45. Roura S, Miravet S, Piedra J, García de Herreros A, Duñach M. Regulation of E-cadherin/catenin association by tyrosine phosphorylation. J Biol Chem 1999, 274: 36734–36740.
46. Niu Y, Wang G, Li Y, Guo W, Guo Y, Dong Z. LncRNA FOXP4-AS1 promotes the progression of esophageal squamous cell carcinoma by interacting with MLL2/H3K4me3 to upregulate FOXP4. Front Oncol 2021, 11: 773864.
47. Christopher AC, Koshy K. Neurological picture. Periventricular heterotopia in refractory epilepsy. J Neurol Neurosurg Psychiatry 2013, 84: 1136–1137.